Predicting Atmospheric Fine Aerosol Concentrations using Multiple Regression Analysis

Project Report (Group 20)
STAT141A Fall Quarter 2020

Andrew T. Weakley, Christina De Cesaris, Zheyuan Walter Yu, Seyoung Jung

December 18, 2020

1 Introduction and Objectives

The Interagency Monitoring of PROtected Visual Environment (IMPROVE) network monitors atmospheric fine particulate matter (*a.k.a.*, $PM_{2.5}$) in US national parks to track long-term trends in air quality and visibility [1]. The National Park Service operates and maintains over 150 aerosol samplers at sites across the contiguous US, Alaska, Hawaii, Virgin Islands, and South Korea (**Figure 1**).

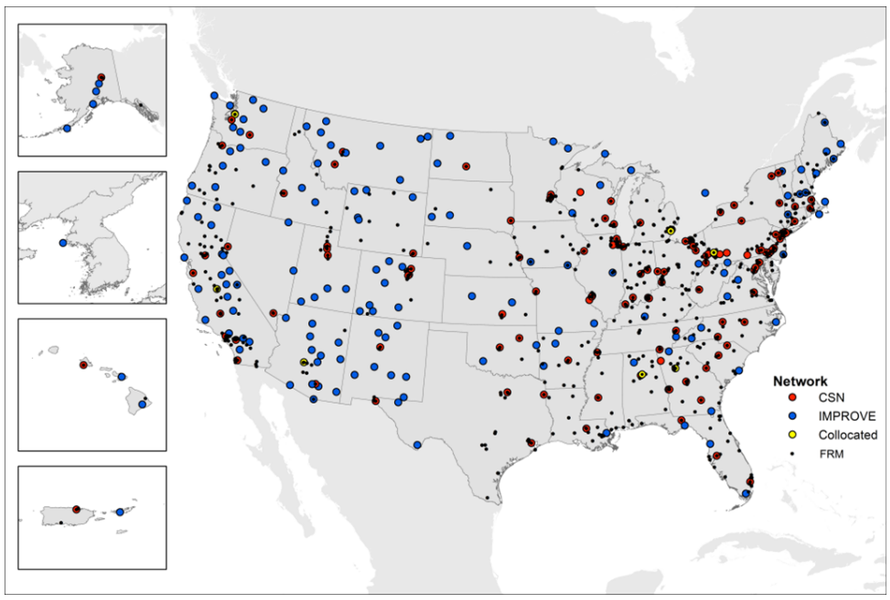

Figure 1: Location of major US particulate monitoring networks. IMPROVE field samplers are denoted as blue dots.

Visibility reduction and the human health impact of $PM_{2.5}$ are related, in a complex way, to both the concentration ($\mu g/m^3$) and composition of atmospheric aerosols [2, 3]. Specifically, variations in regional, seasonal, and local aerosol sources (*e.g.*, summer wildfires in the western US, emission sources related to local industry) obscure a straightforward understanding of the association between total $PM_{2.5}$ collected in the IMPROVE network and the chemical constituents that comprise the aerosol fine mass. Given this, our **first objective** will use publicly available "chemical speciation" records (from the 2015 monitoring year) in a principal component analysis (PCA) to explore the main sources of variability in the speciation data in an effort to attribute variations to emission and aerosol sources.

Our **second objective** will then regresses $PM_{2.5}$ (Y) against the speciation data ($[X]; p <= 32$) using three regression techniques. These methods include multiple linear regression optimized using stepwise variable selection (stepAIC), elastic net regression, and a non-parametric bootstrapped-aggregated (bagged) regression trees [4]. Our **final objective** briefly compares the regression analysis results in the context of the exploratory principal component analysis to judge whether the covariates prioritized for regression analysis may be attributable to emission and atmospheric sources known to compose $PM_{2.5}$ in the IMPROVE network.

2 Methods

2.1 IMPROVE 2015 and Github Repository

Data is made available on the Federal Land Management Database managed by Colorado State University (http://views.cira.colostate.edu/fed/). Exactly 21,501 records (N) containing 92 measurements were downloaded. These data correspond to all IMPROVE monitoring sites. Variables may be divided into the following classes as: aerosol carbon (OC, EC), carbon quality-assurance related (OC1, OC2, OC3, OC4, EC1, EC2, EC3, OP), filter light absorbance (fAbs), anions (NO3, SO4), tracer compounds (Al, As, Br, Ca, Cl, Cr, Cu, Fe, Pb, Mg, Mn, Ni, P, K, Rb, Se, Si, Na, Sr, S, Ti, V, Zn, Zr), species constructs (Soil, SeaSalt, ammNitrate, ammSulfate), and sample identifiers (SiteCode, Date). With the exception of fAbs and sample identifiers, all variables are expressed in units of $\mu g/m^3$. Sample analytical uncertainties (*i.e.*, measurement error as standard deviations) were available for all variables.

Metadata were downloaded with pertinent information concerning field sampler location (state and county) and sampler coordinates (longitude, latitude, elevation).

A Github repository is maintained to share and track changes to the database as well as improve communication between team members (https://github.com/cmdecesaris/stats141A-FinalProject).

2.2 Data Cleaning and Sample Partitioning

2.2.1 Variable selection prior to analysis

Data cleaning determined which variables and samples to include in the subsequent analyses. Variables related to carbon quality assurance (with the exception of OP), chemical constructs, and filter light absorbance were all discarded. OP, a quality-assurance variable, was retained for subsequent regression analyses as it is often used as a tracer for specific sources of $PM_{2.5}$ (*e.g.*, wildfire emissions, diesel particulate matter) [5, 6]. Filter absorbance (fAbs) was also removed as it is a spectroscopic proxy for EC and therefore redundant [7].

Species constructs were removed as they consist of mass-weighted linear combinations of the available tracer variables and subject to several (often strict) assumptions as to their atmospheric sources and composition [8]. For example, the "Soil" construct is calculated using the IMPROVE soil equation as $SOIL = 2.2 * AL + 2.49 * SI + 1.63 * CA + 2.42 * FE + 1.94 * TI$ [9]. Here, each coefficient weights Al, Si, Ca, Fe, and Ti based on the most geologically probable amount of inorganic oxygen bonded to each [10]. Essentially, the soil construct is meant to serve as a "representative/typical" US soil sample and my therefore introduce error into our analyses that might otherwise not exist by using individual tracers alone. Overall, 30 chemical measurements (of the carbon, anion, tracer classes) and 2 categorical variables (SiteCode, Date) were available for regression analysis.[1]

2.2.2 Sample selection

Only samples collected in the contiguous US were considered for analysis to ensure that, to the extent possible, $PM_{2.5}$ was as homogeneous as possible, i.e., identically distributed on a site-to-site basis. Unique site identifiers (SiteCode) from South Korea, Alaska, Hawaii, and the Virgin Islands were therefore identified using IMPROVE metadata. The dplyr filter function then screened sites at those states (and country) from the main array leaving $N = 20629$ records for analysis.[2]

Samples exhibiting inordinately negative $PM_{2.5}$ concentrations were also removed using sample analytical uncertainty (σ_i). As $PM_{2.5}$ can never, in principle, be negative, samples with $PM_{2.5} < -3\sigma_i$ were judged has having a high probability of not being zero (a blank measurement). In other words, negative concentrations outside 3-times analytical uncertainty were more likely the result of systematic as opposed to the random measurement error in $PM_{2.5}$. We should further note that this screening criterion is very conservative as this threshold is approximately 2 times less than reported $PM_{2.5}$ minimum detection limits [11]. After screening other records for missing values, the total number of samples available for analysis was $N = 17294$

2.2.3 Stratified Sample Partitioning

Prior to regression analysis, the data were partitioned into training and testing sets by arranging samples alphabetically by SiteCode and Date variables (MM/DD/2015). Once sorted, the data were

[1] The Soil and Sea Salt constructs did aid exploratory analysis given the pattern of observed loadings.

[2] To address concerns in our project proposal, we decided not to use the percentage of samples below method detection limits as a criterion to select variables for analysis given concerns about censoring. More rational criteria are presented below.

split in half by placing every other sample in the test set, using seq(1,n,2), with $N_{train} = N_{test} = 8647$. Random sampling was eschewed in favor of this approach as pollution data shows seasonality, making it critical that seasonal variability in chemical composition are represented equally in the training and testing sets.

2.3 Exploratory Correlation and Principal Component Analysis

Following sample correlation analysis and visualization using ggcorrplot [12], the main sources of variation within the (non-categorical part of the) predictor matrix were explored with principal component analysis (PCA). Variables were centered, but not scaled, prior to analysis as the subsequent regression analyses were performed on non-standardized covariates. The number of major principle components was selected using a scree plot, aided by the use of statistical aprroaches available in the PCATools package [13]. The first several eigenvectors were plotted to determine if the pattern of loadings were attributable to known aerosol sources. Score plots for the major components were then generated and pseudo-colored on relevant species concentrations to aid interpretation.

2.4 Multiple Regression and stepAIC optimization

A first-order multiple regression used the lm() function to regress half the $PM_{2.5}$ (Y) measurements against the 30 speciation measurements ([X]; N_{train}=8647, p=30). Assumptions of linearity, normality and homoscedasticity were checked based on the residual plots, normal Q-Q plots, and Box-Cox procedure. Forward selection, backward elimination, forward stepwise, and backward stepwise selection were toggled in the stepAIC function and each explored as a means of model optimization. The AIC and BIC were then used to selected the "best" eight candidate models according to these criteria. Model validation then used the test data (N_{test}=8647) to select a final model according to overall prediction ability (e.g., RMSE,R^2), consistency between training and testing set performance, and the principle of parsimony (Occam's razor).

2.5 Elastic Net Regression Analysis

Elastic net regression proceeded in a manner similar to lm() fitting, using the cv.glmnet() function available in the glmnet package [14]. Elastic net is appealing for our purposes given that biased estimators typically show better out-of-sample prediction performance than unbiased linear estimators [4]. Specifically, elastic net regression minimizes the least squares objective function (SSE) subject to a LASSO and ridge penalty as

$$\hat{\beta} = \underset{\beta}{argmin}\Big\{ \sum_{i=1}^{N}(y_i - \beta_0 - \sum_{j=1}^{p} x_{ij}\beta_j)^2 + \lambda \sum_{j=1}^{p}(\alpha\beta_j^2 + (1-\alpha)|\beta_j|\Big\} \tag{1}$$

where β_j are the p regression coefficients, x_{ij} are the p predictors, λ is the regularization penalty, and α is the elastic net penalty [4]. Elastic net regression balances fidelity to the full-predictor ridge solution ($\alpha = 1$) and the sparse-variate LASSO regression ($\alpha = 0$), the later performing subset selection during estimation.

In practice, the user must specify λ and α. In this study, ten-fold cross validation was used to find the optimal values for λ for 20 different values of α. The mean squared error of prediction (MSEP) was used to evaluate the best model.

2.6 Bagged Regression Trees

Decision tree regression analysis was carried out using the rpart and caret package [15, 16]. Decision trees are highly interpretive flow chart models useful for predicting data based on a series of binary splits constructed through the training data. As a result, decision trees are subject to high variability between models given the same data set. For a single tree model, the training data was partitioned using 10-fold cross validation process to optimize the model. The optimal hyper-parameters were evaluated through grid search and determined based on which resulted in the lowest validation error and Mallow's C_p.

To combat the high variability produced by a single tree model, a tree bagging ensemble method was employed utilizing the caret package. In this process, random subsets of the training data are selected with replacement and used to build a ensemble of different tree models. The predictive ability of the bagged regression tree model is the average perform ace of all trees within that model.

3 Results and Discussion

3.1 Exploratory Analysis

Figure 2 (LHS) shows a plot of the species sample correlations where their axis labels have been organized using the agglomerative hierarchical clustering option in the ggcorrplot function. Notably, the position and clustering of the variables on the correlation plot makes sense given the sources of aerosol most likely impacting IMPROVE samples. Beginning from the bottom left and working to the top right, we see that MG, CL, and NA cluster together and are highly correlated. These species are all good tracers for marine aerosols (sea spray) [17, 18]. Next, we see that carbon species (OC,EC,OP) cluster with $PM_{2.5}$. This likely indicates that carbon comprises as a large amount of $PM_{2.5}$ mass. Indeed, we see that OC, and to a lesser extent EC and OP, comprise a large amount of sample mass in in these samples (on average; see **Figure 2 (RHS)**). Continuing further, we see that species attributable with soil (Al,Si,Fe,Ti), shipping (Ni,V), coal combustion (Se,S,SO4), and incinerator sources (Pb,Zn) all cluster together [9, 19, 17].

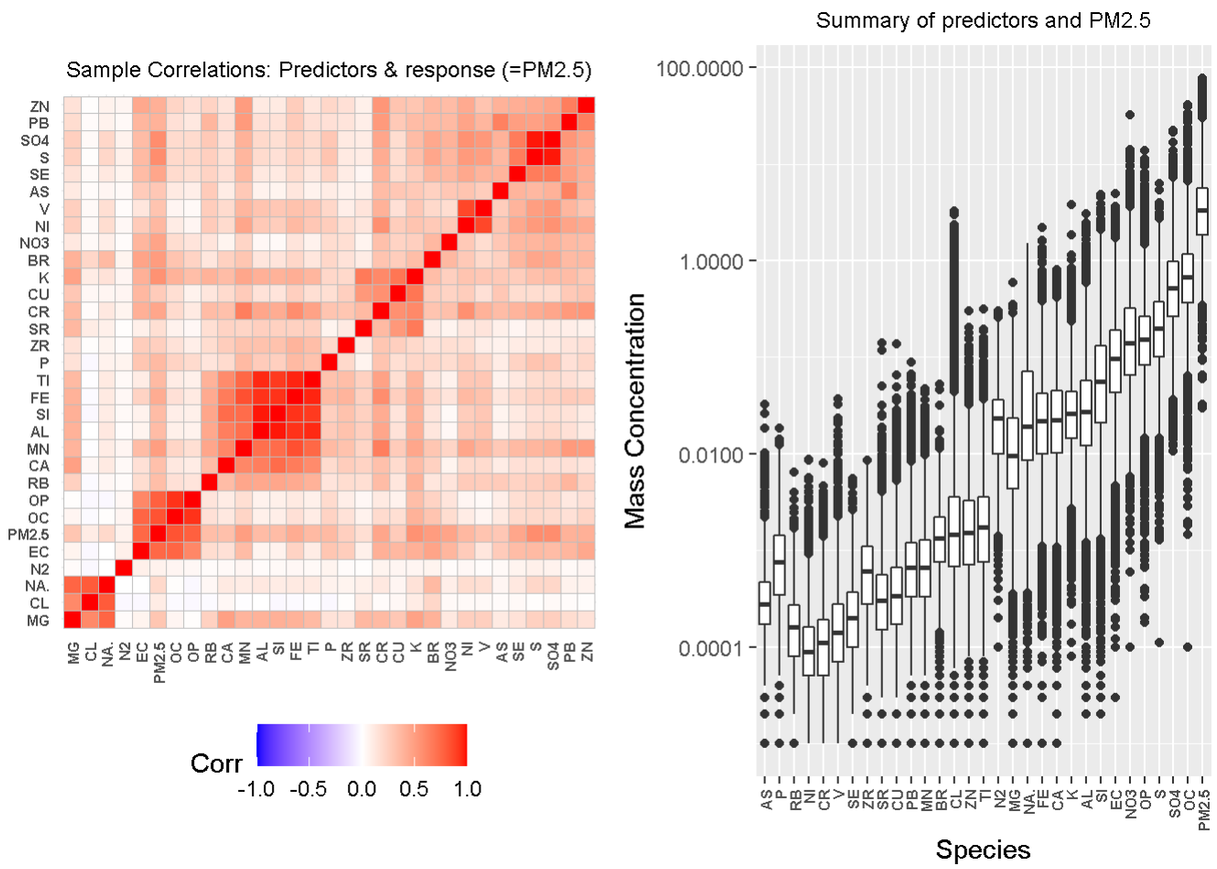

Figure 2: Correlation Matrix and Boxplots of Species comprising $PM_{2.5}$, sorted in order of least mass contribution

Figure 3 shows a scree plot of the individual and cumulative amount of variance explained the in predictor matrix. Here, we see that the first 3 components explain over 95% of the variance in the data. Depending on the component selection method used, 3 to 4 components were considered appropriate to model the data.

After interpreting the principal component loadings (see supplemental material), it was determined that the first and second principal components were likely modeling variance related to organic carbon (OC) and total anion concentration (SO4+NO3) respectively. **Figure 4** shows the sample observations projected onto the first two components, colored according to OC and total anion content, respectively.

Repeating the procedure indicated that the 3rd and 4th components were modeling a rough contrast between NO3 and SO4 (PC3) and soil impacts (see Section S1 in Supplemental Material). Additionally, PC5 and PC6 (more roughly) modeled OP and marine aerosol impacts (see Supplemental Material). Notably, the clear interpretation of the components was directly proportional to the amount of variance explained by each.

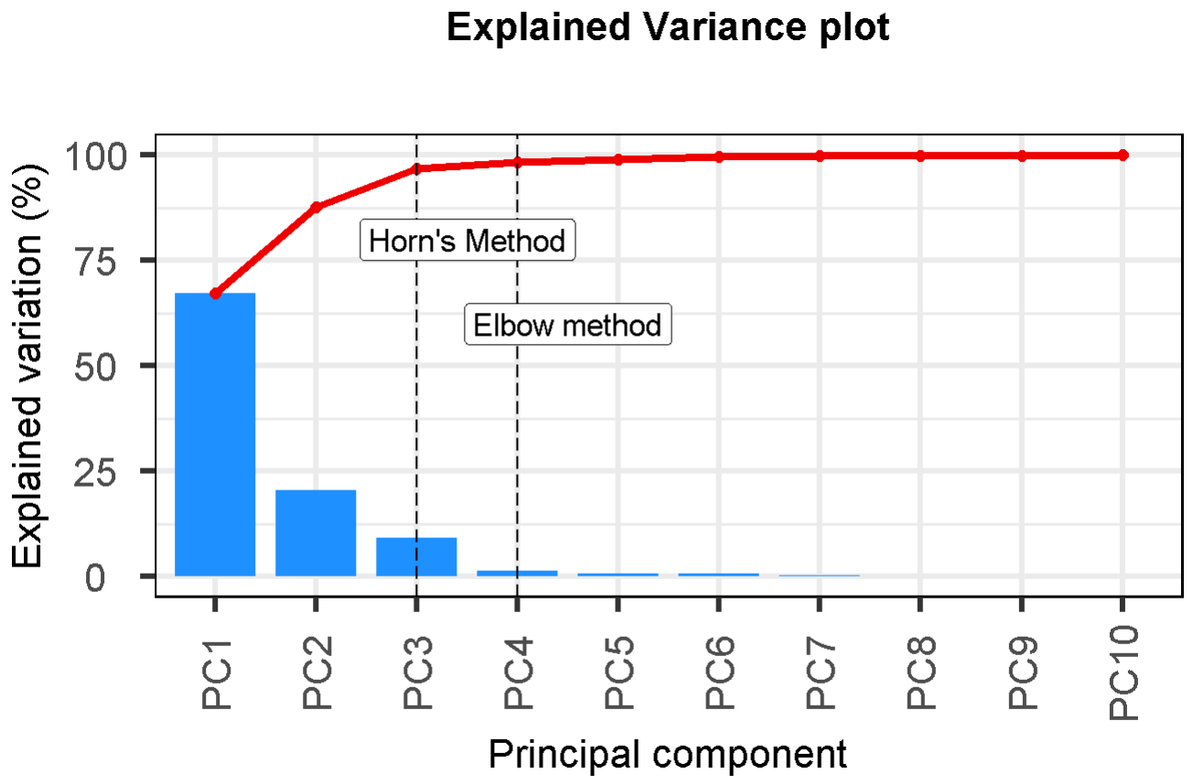

Figure 3: Principal component scree plot

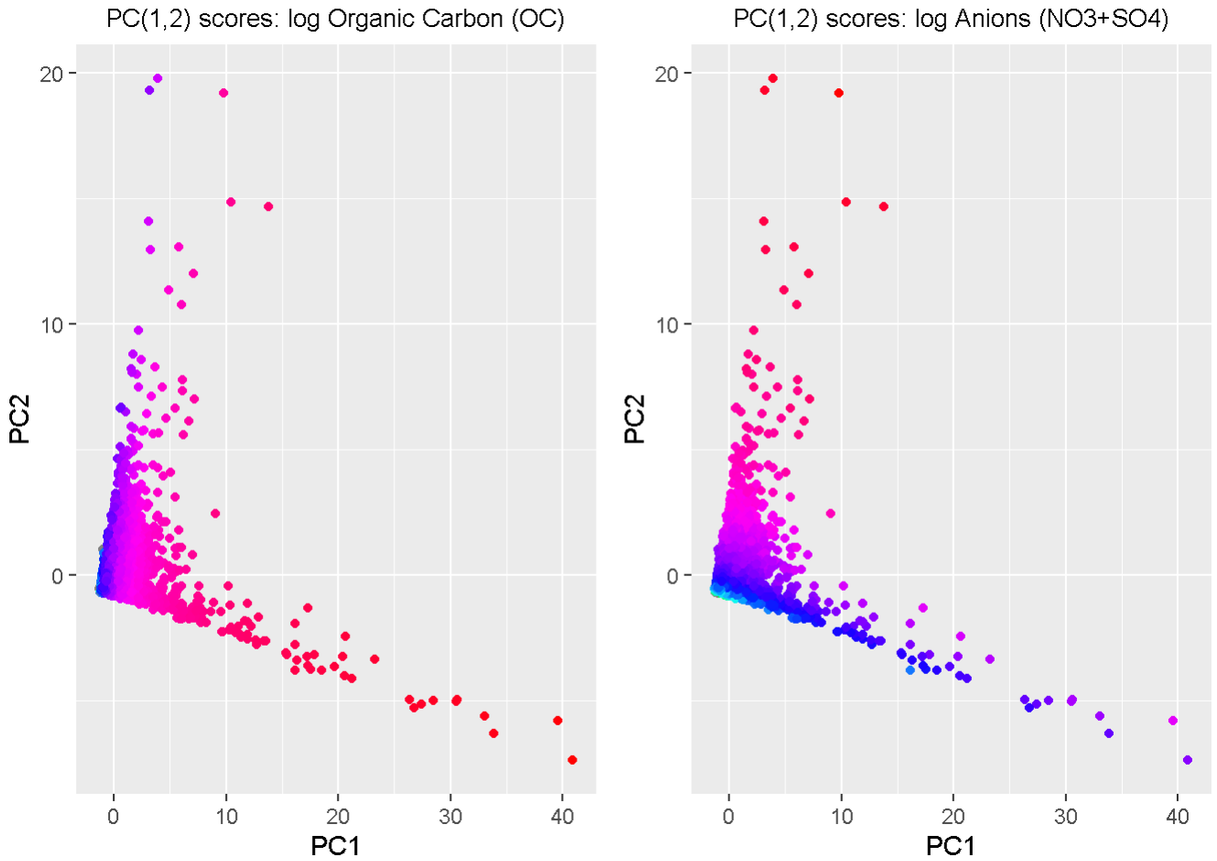

Figure 4: Principal component 1-2 subspace colored on log species concentrations. Blue denotes low species' concentration while magenta denotes higher concentration. log scaling was used to promote contrast.

3.2 Regression analysis

3.2.1 Multiple Regression and stepAIC optimization

Based on residual plots, normal q-q plots, and a Box Cox procedure applied to the eight best stepAIC models, the assumptions of linearity, normality, and homoscedasticity are all valid (see Supplemental Material for details). First, it was interesting that all of these models had very good prediction ability. The R-square values, representing the "variance explained" between the predicted and observed test set values, were very high in these models ($R^2 > 0.977$). The root mean squared error, a measure of the average prediction error made by the model in predicting the outcome for an observation, were very low in all models ($RMSEP < 0.773/m^3$).

The consistency between the models from training data and testing data were also compared. The regression coefficients were very consistent between training data and testing data, because they had the same signs and the similar values.

At the end, the Occam's razor principle was ultimately used to determine the final models. Model 5 and model 7 had the least number of regression coefficients, so they were selected; in fact, these two models were actually the same upon further inspection. Notably, model 5 was selected by forward selection based on BIC, and model 7 selected by forward stepwise based on BIC.[3] The model is given below as:
PM2.5 = - 0.2068 + 1.9302*OC + 0.4269*SO4 + 2.2615*FE + 1.2239*NO3 +
3.5397*CL + 2.9903*SI + 3.8678*S + 2.4363*K + 1.9114*CA - 29.5285*CU +
24.5011*PB + 47.1501*P + 0.2289*OP + 18.4563*TI + 141.3513*SE

3.2.2 Elastic Net Regression

After converting the factor variables (SiteCode and Date) to dummy variables, the training set will have 308 variables (30 + 278 factor levels). Ten-fold cross validation for 20 different values for α (between 0 and 1) was fitted using cv.glmnet. The the test set mean squared error for each fit is given (**Table 1**).

Table 1: Test set MSE for each *alpha* considered by 10-fold CV

Alpha	MSE	Alpha	MSE
0.00	0.7634257	0.55	0.6141631
0.05	0.6054706	0.60	0.6186419
0.10	0.6065652	0.65	0.6227428
0.15	0.6123570	0.70	0.6171354
0.20	0.6071487	0.75	0.6373969
0.25	0.6166402	0.80	0.6155697
0.30	0.6084149	0.85	0.6355489
0.35	0.6113124	0.90	0.6405099
0.40	0.6070638	0.95	0.6545169
0.45	0.5977094	1.00	0.6332386
0.50	0.6352535	-	-

In Table 1, we can see that neither ridge Regression nor LASSO Regression ($\alpha = 0$) gives us the best result. Although both models given very similar results in terms of MSE, the lowest MSE is achieve from α=0.45. Since we are using elastic net Regression, we can expect that this model has fewer predictor variables than the full model (but likely more than the suboptimal LASSO solution). For the model with α=0.45, cross validation chose a λ=0.074.

Indeed, **Table 2** indicates that 52 out of the original 308 variables are nonzero indicating that most of the variables are not useful to the regression problem.

[3]Comprehensive analysis details in Section S2 of supplemental material

Table 2: Elastic net regression coefficients for $(\lambda, \alpha) = (0.074, 0.45)$

Variable	Coefficient	Variable	Coefficient	Variable	Coefficient
(Intercept)	-0.114674053	TI	9.062758625	Date6/11/2015	0.284272033
EC	0.426403466	V	18.565709821	Date6/23/2015	0.044890657
OC	1.711304246	NO3	1.178011209	Date6/29/2015	0.054805817
OP	0.807417478	SO4	0.618401342	Date7/2/2015	0.318254665
AL	0.971613825	SiteCodeCORI1	-0.010450120	Date7/29/2015	0.186479582
BR	12.595389511	SiteCodeELDO1	-0.136389716	Date7/5/2015	0.026638887
CA	1.756914687	SiteCodeMAKA2	0.002197642	Date8/10/2015	0.003149496
CL	2.745861899	SiteCodeMAVI1	0.088369079	Date8/13/2015	0.003635989
FE	3.510792738	SiteCodePHOE1	-0.127508792	Date8/16/2015	0.157029484
PB	8.392527873	SiteCodePORE1	0.660387523	Date8/19/2015	0.288633654
MG	1.062569693	SiteCodeREDW1	0.017723498	Date8/25/2015	0.227724937
P	27.117590226	SiteCodeSAGA1	-0.103433378	Date8/28/2015	0.222549734
K	1.768529297	SiteCodeSAMA1	0.074553728	Date8/31/2015	0.123963928
RB	85.508506989	Date3/13/2015	-0.011986774	Date8/4/2015	0.195171963
SE	127.200123974	Date3/19/2015	-0.026328360	Date8/7/2015	0.147065416
SI	2.285695803	Date3/22/2015	-0.076507845	Date9/18/2015	0.027475458
NA	0.362930418	Date3/4/2015	-0.009827235	Date9/3/2015	0.091789732
S	3.102419694	Date3/7/2015	-0.258708631	-	-

Notably, many of the chemical and tracer variables (21 out of 30) remain in the model.[4] However, a majority of the SiteCode factor levels are dropped and half of their coefficient values are negative. Furthermore, we can see that the selected Date levels are mostly from the summer season (from June to August). This is likely due to the higher PM concentrations in the summer months (At some sites) due to wildfires [20]. At first glance, it interesting to see that a few of the selected variables, such as SE (Selenium), RB (Rubidium), P (Phosphorous) and BR (Bromine), have extremely larger coefficient values compared to the others. However, as shown in **Figure 1** these variables comprise a very small amount of the total mass of $PM_{2.5}$, approximately two orders of magnitude less than OC and SO4 for example. They are therefore given largest coefficients to account for this difference in scale.

3.2.3 Bagged Regression Trees

After performing grid search for tree fitting, the optimal single (non-bagged) tree model had a c_p of 0.1, a minimum split of 10, and a maximum depth of 8. The optimal tree had a RMSE of 2.156 $\mu g/m^3$, an R Squared Value of 0.83, and an MAE of 1.21 $\mu g/m^3$. A graphical depiction of the model is presented in **Figure 6**.

The graphical depiction of the bagged tree model is complex and difficult to show. The final model consisted of 25 tree models, had an RMSE of 1.80 $/m^3$, an R Squared Value of 0.875, and MAE of 0.958 $/m^3$. The bagged tree model was used to plot predictors by importance, normalized to the most important. The most important predictor was carbon, followed by OP, and Potassium. The full break down is presented in **Figure 7**.[5]

[4]Comprehensive analysis details in Section S3 of supplemental material
[5]Comprehensive analysis details in Section S4 of supplemental material

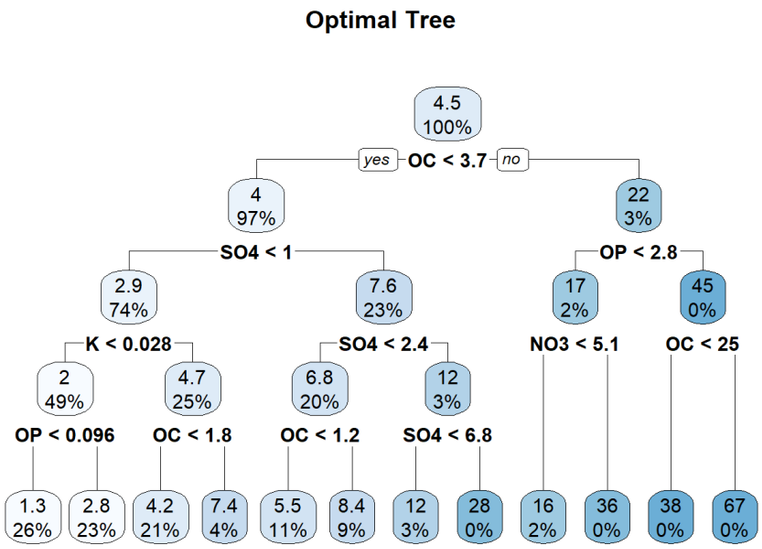

Figure 5: Optimal Decision Tree

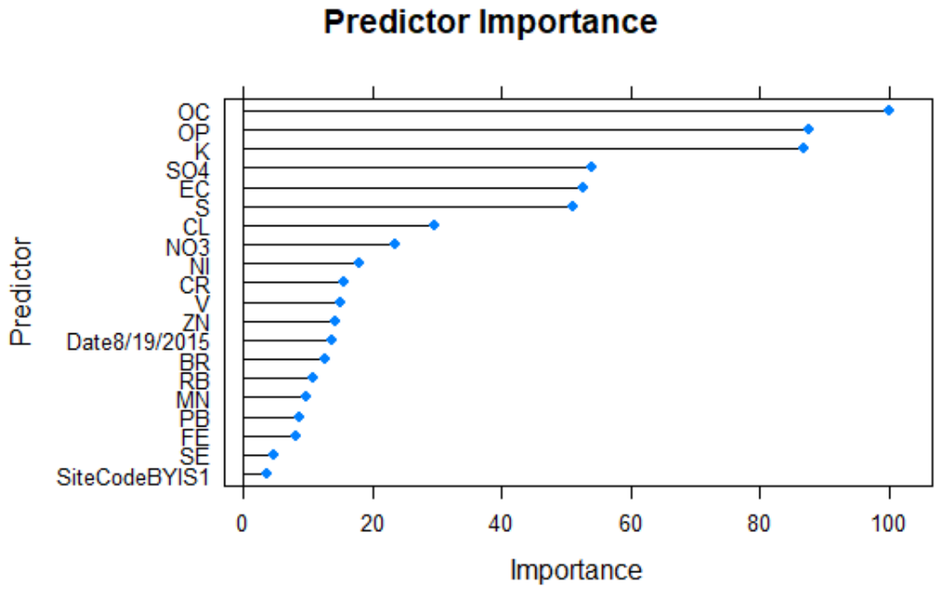

Figure 6: Optimal Decision Tree

4 Conclusions: Model comparison and source attribution

The prediction of $PM_{2.5}$ varied by model and method with test set R^2 ranging from 0.875 in the case of bagged regression trees to as high as 0.977 for multiple regression. Irrespective of the relative prediction performance of each model, we see that they all tended to prioritize very similar covariates. Specifically, carbon predictors (OC,EC,OP) were used in all regressions, with the importance of OC occupying the top spot in both the multiple regression and regression tree following optimization. Furthermore, SO4, OP, and NO3 also occupied principal positions in linear regression and bagged tree. Such results make sense in the context of Figure 1: the principal source of variance in the predictor matrix are from OC and anion content (NO3+SO4).[6]

One notable difference between the parametric regressions (*i.e.*, multiple regression and elastic net) and the regression tree is the former's reliance on carbon and soil-related species (Ca,Si,Ti) while the latter used no tracers for soil species. This reason my have contributed to the regression tree's less-optimal performance when judged against the other models. Overall, all models appear reasonable for the prediction of PM2.5 in the IMPROVE network.

[6]It should be noted that $OC = OC1 + OC2 + OC3 + OC4 + OP$ and $EC = EC1 + EC2 + EC3 - OP$. OP was included in the model as an empirical factor to adjust for potential biases related to OC/EC thermal analysis [21].

References

[1] Paul A. Solomon et al. "U.S. National PM2.5 Chemical Speciation Monitoring Networks—CSN and IMPROVE: Description of networks". In: *Journal of the Air Waste Management Association* 64.12 (2014), pp. 1410–1438. ISSN: 1096-2247. DOI: 10.1080/10962247.2014.956904.

[2] John G Watson. "Visibility: Science and regulation". In: *Journal of the Air Waste Management Association* 52.6 (2002), pp. 628–713. ISSN: 1096-2247.

[3] Cliff I. Davidson, Robert F. Phalen, and Paul A. Solomon. "Airborne Particulate Matter and Human Health: A Review". In: *Aerosol Science and Technology* 39.8 (2005), pp. 737–749. ISSN: 0278-6826. DOI: 10.1080/02786820500191348.

[4] T. Hastie, R. Tibshirani, and J. Friedman. *The Elements of Statistical Learning: Data Mining, Inference, and Prediction*. Springer Series in Statistics. Springer New York, 2013.

[5] B. Khan et al. "Differences in the OC/EC ratios that characterize ambient and source aerosols due to thermal-optical analysis". In: *Aerosol Science and Technology* 46.2 (2012), pp. 127–137. DOI: 10.1080/02786826.2011.609194.

[6] Andrew T. Weakley et al. "Ambient aerosol composition by infrared spectroscopy and partial least squares in the chemical speciation network: Multilevel modeling for elemental carbon". In: *Aerosol Science and Technology* 52.6 (2018), pp. 642–654.

[7] Warren H. White et al. "A critical review of filter transmittance measurements for aerosol light absorption, and de novo calibration for a decade of monitoring on PTFE membranes". In: *Aerosol Science and Technology* 50.9 (2016), pp. 984–1002. ISSN: 0278-6826. DOI: 10.1080/02786826.2016.1211615.

[8] JudithC Chow et al. "Mass reconstruction methods for PM2.5: a review". In: *Air Quality, Atmosphere Health* 8.3 (2015), pp. 243–263. ISSN: 1873-9318. DOI: 10.1007/s11869-015-0338-3.

[9] J. L. Hand et al. "Trends in remote PM2.5 residual mass across the United States: Implications for aerosol mass reconstruction in the IMPROVE network". In: *Atmospheric Environment* 203 (2019), pp. 141–152. ISSN: 1352-2310. DOI: https://doi.org/10.1016/j.atmosenv.2019.01.049.

[10] William C. Malm et al. "Spatial and seasonal trends in particle concentration and optical extinction in the United States". In: *Journal of Geophysical Research: Atmospheres* 99.D1 (1994), pp. 1347–1370. DOI: doi:10.1029/93JD02916.

[11] Analytical Methods Committee. "Recommendations for the definition, estimation and use of the detection limit". In: *Analyst* 112.2 (1987), pp. 199–204.

[12] Alboukadel Kassambara. *ggcorrplot: Visualization of a Correlation Matrix using 'ggplot2'*. R package version 0.1.3. 2019. URL: https://CRAN.R-project.org/package=ggcorrplot.

[13] Kevin Blighe and Aaron Lun. *PCAtools: PCAtools: Everything Principal Components Analysis*. R package version 2.2.0. 2020. URL: https://github.com/kevinblighe/PCAtools.

[14] Noah Simon et al. "Regularization Paths for Cox's Proportional Hazards Model via Coordinate Descent". In: *Journal of Statistical Software* 39.5 (2011), pp. 1–13.

[15] Terry Therneau and Beth Atkinson. *rpart: Recursive Partitioning and Regression Trees*. R package version 4.1-15. 2019. URL: https://CRAN.R-project.org/package=rpart.

[16] Max Kuhn. "Building Predictive Models in R Using the caret Package". In: *Journal of Statistical Software, Articles* 28.5 (2008), pp. 1–26. ISSN: 1548-7660. DOI: 10.18637/jss.v028.i05. URL: https://www.jstatsoft.org/v028/i05.

[17] Xin-Hua Song, Alexandr V. Polissar, and Philip K. Hopke. "Sources of fine particle composition in the northeastern US". In: *Atmospheric Environment* 35.31 (2001), pp. 5277–5286.

[18] Li-Jun Zhao et al. "Magnesium Sulfate Aerosols Studied by FTIR Spectroscopy: Hygroscopic Properties, Supersaturated Structures, and Implications for Seawater Aerosols". In: *The Journal of Physical Chemistry A* 110.3 (2006), pp. 951–958. ISSN: 1089-5639. DOI: 10.1021/jp055291i.

[19] Mar Viana et al. "Impact of maritime transport emissions on coastal air quality in Europe". In: *Atmospheric Environment* 90 (2014), pp. 96–105.

[20] D. M. Murphy et al. "Decreases in elemental carbon and fine particle mass in the United States". In: *Atmospheric Chemistry and Physics* 11.10 (2011), pp. 4679–4686.

[21] Judith C Chow et al. "The DRI thermal/optical reflectance carbon analysis system: description, evaluation and applications in US air quality studies". In: *Atmospheric Environment. Part A. General Topics* 27.8 (1993), pp. 1185–1201. ISSN: 0960-1686.